



# Magnetic energy release and topology in solar active phenomena

C.H. Mandrini<sup>1,2</sup>

<sup>1</sup> *Instituto de Astronomía y Física del Espacio, CONICET-UBA, Argentina*

<sup>2</sup> *Facultad de Ciencias Exactas y Naturales, UBA, Argentina*

*Contact / mandrini@iafe.uba.ar*

**Resumen** / La energía liberada durante los eventos activos, que ocurren en la atmósfera solar, está contenida en las corrientes asociadas al campo magnético que ha emergido luego de atravesar la zona convectiva. Una vez que el flujo magnético alcanza la fotosfera, el mismo puede ser forzado aún más a través de los movimientos en esta capa atmosférica inferior. Se acepta, en general, que la reconexión magnética es el mecanismo a través del cual la energía magnética almacenada se transforma en energía cinética de partículas aceleradas y flujos de masa y energía radiativa a lo largo de todo el espectro electromagnético. Aunque este mecanismo es eficiente sólo en escalas espaciales muy pequeñas, el mismo puede implicar una reestructuración a gran escala del campo magnético; esta reestructuración se puede inferir del análisis combinado de las observaciones, el modelado del campo coronal y el cálculo de su topología. Los eventos resultado de la liberación de energía van desde nanofulguraciones, aún indetectables a la resolución espacial de las observaciones actuales, a poderosas fulguraciones, que pueden ir acompañadas de la expulsión de grandes cantidades de plasma y campo magnético en eventos llamados eyecciones coronales de masa (CMEs), y fenómenos estacionarios como el viento solar lento. En este trabajo discutiremos cómo el cálculo y análisis de la topología del campo magnético, aplicada a la variedad más amplia de configuraciones magnéticas observadas, se puede utilizar para identificar las zonas de liberación de energía y sus características físicas.

**Abstract** / The energy released during active atmospheric events in the Sun is contained in current-carrying magnetic fields that have emerged after traversing the solar convective zone. Once the magnetic flux reaches the photosphere, it may be further stressed via motions in this lower atmospheric layer. Magnetic field reconnection is thought to be the mechanism through which the stored magnetic energy is transformed into kinetic energy of accelerated particles and mass flows, and radiative energy along the whole electromagnetic spectrum. Though this mechanism is efficient only at very small spatial scales, it may imply a large-scale restructuring of the magnetic field which is inferred from the combined analysis of observations, models of the coronal magnetic field, and computation of its topology. The consequences of energy release include events that range from nano-flares, still below our present observational spatial resolution, to powerful flares that may be accompanied by the ejection of large amounts of plasma and magnetic field in events called coronal mass ejections (CMEs), and stationary phenomena like the slow solar wind. We will discuss how the computation and analysis of the magnetic field topology, applied to the widest variety of observed magnetic configurations, can be used to identify the energy release locations and their physical characteristics.

*Keywords* / Sun: magnetic field — Sun: magnetic topology — Sun: flares — Sun: coronal mass ejections (CMEs)

## 1. Introduction

It is generally admitted that the energy released in solar active phenomena is taken from the magnetic field energy where the event occurs. However, a potential magnetic field is a minimum energy state and cannot be the source of the released energy. Therefore, free magnetic energy has to be accumulated in the non-potential part of the field in the form of electric currents flowing in the solar atmosphere. How and where this energy is released may greatly depend on the connectivity of the magnetic field lines in the corona (i.e. its topology). The earliest works connecting the topology of a magnetic field with flux systems separated by magnetic field lines in 2D (and surfaces in 3D) were the ones of Sweet (1958, 1969). A magnetic null point is present at the intersection of these field lines. Sweet suggested

that a current, when formed, should be centered at this intersection. In 3D surfaces, separatrices are present instead of field lines and the intersection of these surfaces is a line, called the separator. It was shown that the separator is a singular line where the frozen-in condition does not apply and electric currents could flow (see works as early as Syrovatskii, 1981). Separatrix surfaces divide the magnetic volume into topologically distinct regions, in the sense that any of them contains only field lines that start at a particular magnetic flux source and end up at another particular flux source (see Figure 1 in Mandrini et al., 1991). When magnetic reconnection occurs, magnetic flux is transferred from one region to another and magnetic energy can be released (see e.g. the review work by Longcope, 2005, and references therein). A large number of articles invoked this 3D topological scenario to interpret solar flares and

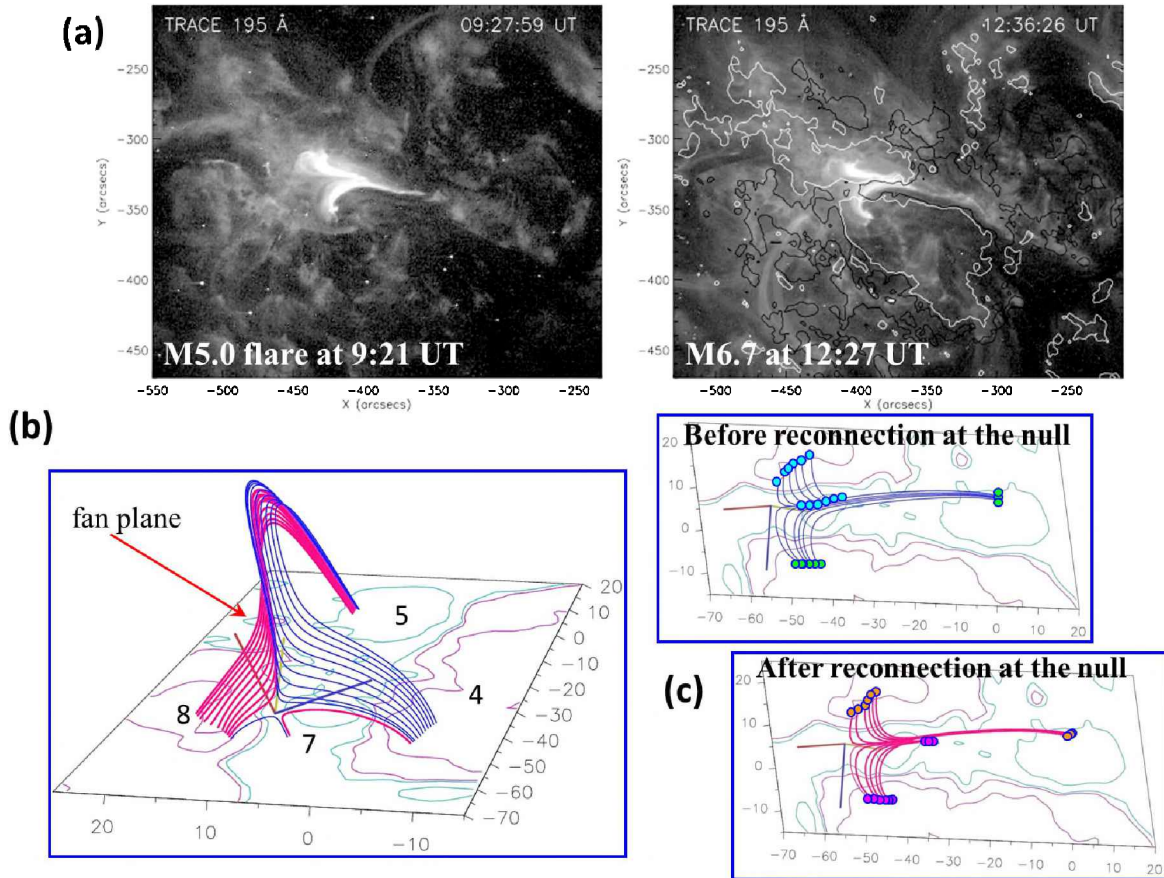


Figure 1: (a) Transition Region and Coronal Explorer (TRACE) images in 195 Å showing the flare loop brightenings at coronal level of both M-class flares. A Michelson Doppler Imager (MDI) magnetogram (at 12:47 UT) isocontour of  $\pm 100$  G (white/black continuous line corresponds to the positive/negative field value) has been overlaid on the image on the right as reference. The field of view is the same in both panels. (b) Shows the magnetic null point location in AR 10486 coronal field from a 3D perspective. The null point height is 3.1 Mm. Field lines in this panel have been computed starting integration at finite distances from the null. A set of blue continuous lines follow roughly the direction of the eigenvector with the lowest eigenvalue in the fan plane. These have footpoints at polarities 4 and 5. These field lines could reconnect at the null with field lines linking 7 to 8, these are represented by only one short blue continuous line. After reconnection, we would have the set of red continuous field lines that have footpoints at 8 and 5 and those that connect 4 and 7 (the latest are represented by only one short continuous field line). The three eigenvectors of the Jacobian field matrix have been depicted at the null location. (c) Coronal magnetic field model of AR 10486 close to the magnetic null. The top and bottom panels show the field lines drawn in (b) in the observer's point of view before and after reconnection. Notice that the shape of these lines follows closely the shape of TRACE loops. Several short field lines have been added as compared to those in (b). We also depict the location of the null. In (b) and (c) the negative/positive field isocontours are shown in continuous magenta/cyan thin lines, their values are  $\pm 100, 1000$  G. The axes are labeled in Mm. Adapted from Luoni et al. (2007).

other energetic phenomena and found that flare brightenings were located at the intersection of separatrices with the photosphere as a proof of magnetic energy release (Gorbachev & Somov, 1988, 1989; Mandrini et al., 1991, 1993; Démoulin et al., 1994; Bagalá et al., 1995; Longcope, 1996). In all these examples, and the ones we will discuss later, magnetic reconnection is understood as a change in magnetic connectivity through which the magnetic configuration goes from a higher energy state to a lower one with the consequent release of energy. The coronal magnetic field was at first modelled using sub-photospheric sources to represent the photospheric flux concentrations (see the review by Mandrini et al., 1997) and later a force-free approach was used, in

all cases the observed photospheric magnetic field was taken as boundary condition (see e.g. Mandrini et al., 1996; Démoulin et al., 1997).

Other topological structures, apart from null points, where the magnetic field connectivity is discontinuous are the so-called bald patches or BPs (Titov et al., 1993). At a BP the field lines are curved upward and the horizontal component of the magnetic field crosses the photospheric inversion line (PIL) from the negative to the positive polarity (i.e. in the opposite way when compared to normal portions of the PIL). Bald patches define separatrices where current layers can develop (see e.g. Vekstein et al., 1991; Aly & Amari, 1997). More recently, Pariat et al. (2009) showed that currents

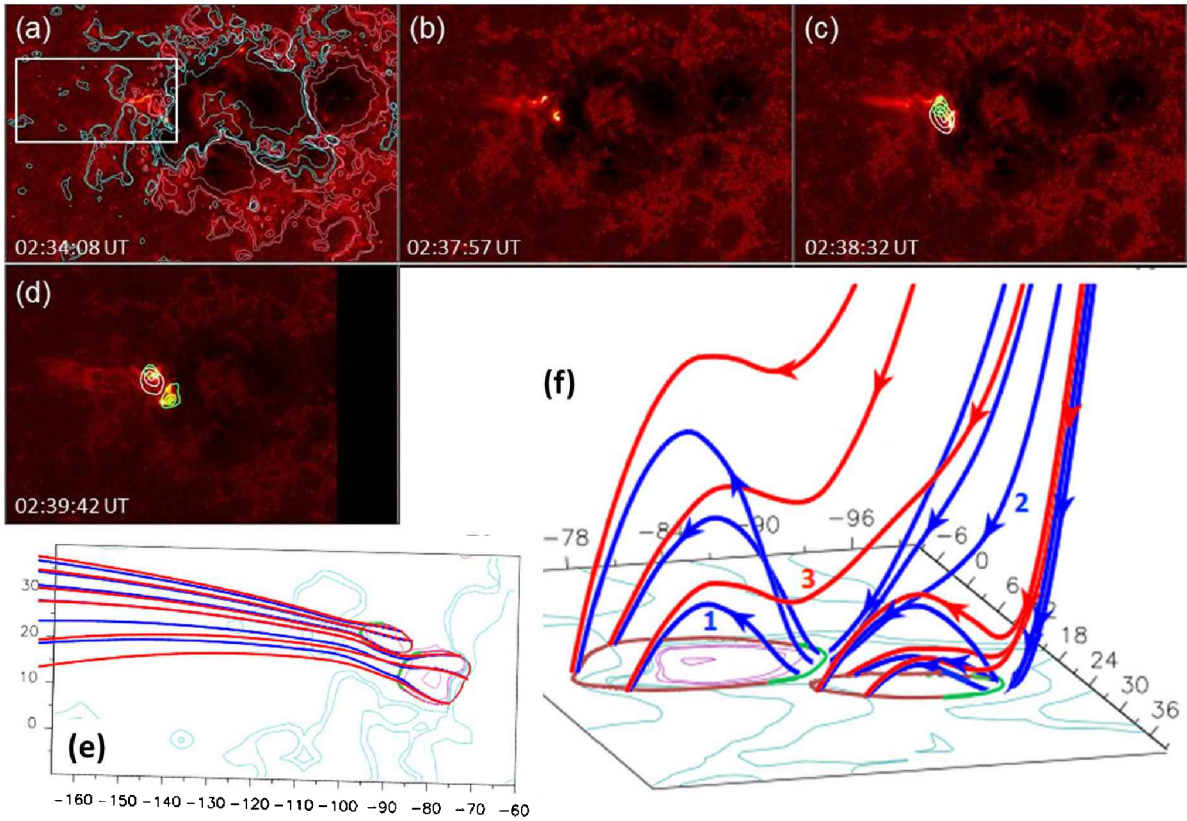


Figure 2: (a, b, c, d) Sequence of TRACE 1700 Å images, showing the blowout jet and the M2.4 flare on 23 October 2003, overlaid by cotemporal Reuven Ramaty High-Energy Solar Spectroscopic Imager (RHESSI) X-ray contours. The yellow/light-green contours correspond to the 10–15/50–100 keV range. MDI isocounters of  $\pm 50, 100, 500$  G (magnetogram at 01:35 UT) have been overlaid to panel (a), shown in continuous magenta/cyan line for positive/negative field. The white rectangle in panel (a) indicates the FOV shown in panel (e). (e) Magnetic field model showing the two BPs found in the AR configuration and a set of pre-reconnected and reconnected field lines as inferred when comparing with observations. The blue solid lines would correspond to the situation before reconnection, while the set of red continuous lines issued from the BP separatrices, located at the photospheric level, would correspond to the lines after reconnection. This panel is shown from the observer point of view. (f) This is the same set of field lines as in panel (e) drawn from a different 3D perspective so that the field connectivity becomes clear. We have also added arrows to the computed lines to indicate the direction of the magnetic field and numbers to some of them to explain how reconnection can proceed (1 would reconnect to 2 and give 3). The height of these field lines was multiplied by a factor of four so that they can be clearly distinguished. Notice the agreement between the reconnected field lines and the shape and direction of the jet, as well as the location of flare kernels on the BP separatrices. The conventions for the field isocontours are as in panel (a). The axes are in Mm. BPs are shown as thick green continuous lines, while the magenta thick continuous lines correspond to the photospheric trace of BP separatrices. Adapted from Chandra et al. (2017).

can accumulate at BPs and their separatrices in magnetohydrodynamic (MHD) numerical simulations. Other simulations like those by Archontis & Hood (2013) or Takasao et al. (2015) have shown the development of magnetic reconnection at BPs during the build up of active regions (ARs).

However, after computing the magnetic topology of a large number of magnetic configurations with various boundary magnetic field distributions (from quadrupolar to bipolar ARs with an S-shaped PIL and even with a nearly potential field and an almost straight PIL), it was found that the presence of magnetic nulls or BPs was not a necessary condition for having an active event and that, in some cases, if a null was present, it could be at any place along the separator and not necessarily related to the region where the energy was released

(see e.g. Démoulin et al., 1994; Schmieder et al., 2007). These results and theoretical developments aiming to understand magnetic reconnection in 3D led Démoulin et al. (1996) to propose that magnetic reconnection may occur in the absence of null points at quasi-separatrix layers (QSLs). These are 3D thin volumes where the coronal field-line connectivity experiences a drastic change. QSLs are preferred sites for the formation of current layers and are therefore locations where magnetic reconnection is prone to occur. Several numerical experiments support this idea (see e.g. Milano et al., 1999; Aulanier et al., 2005; Pariat et al., 2006; Wilmot-Smith et al., 2009; Effenberger et al., 2011; Savcheva et al., 2012; Janvier et al., 2013).

In Sec. 2. we will show examples of observed magnetic configurations in which the magnetic connectivity

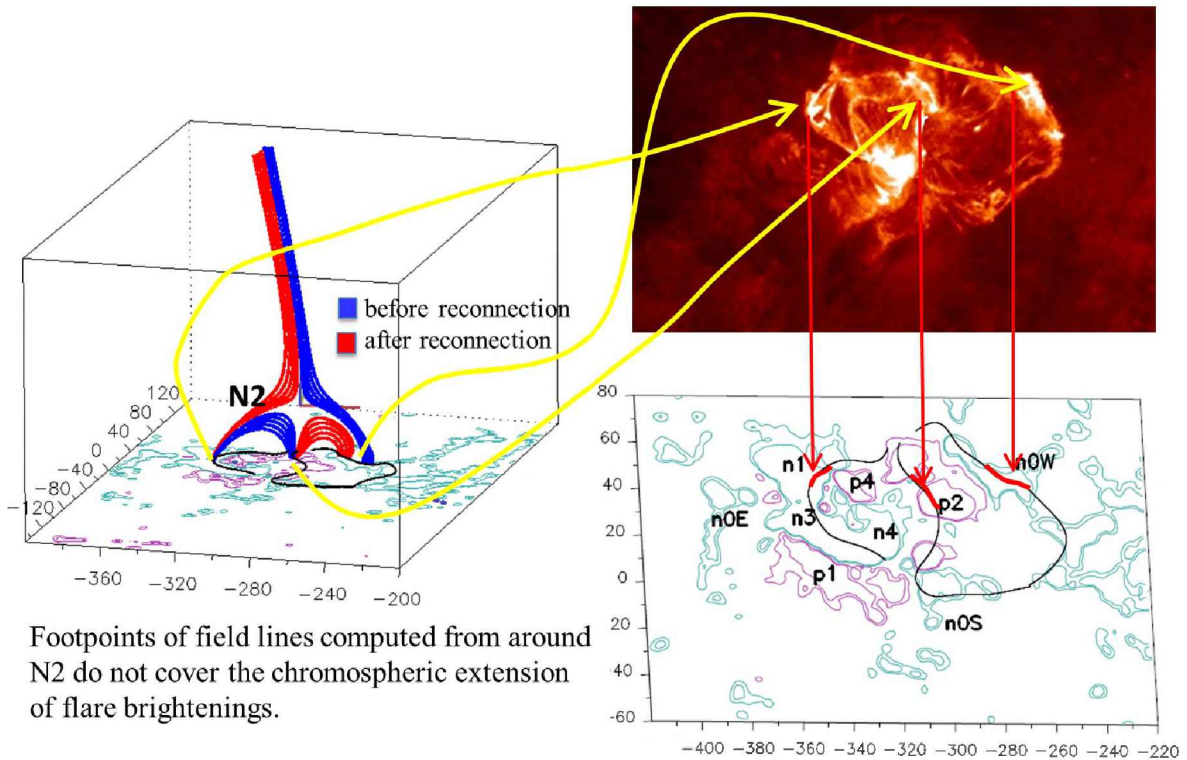


Figure 3: Coronal magnetic-field model in the close vicinity of a magnetic null point, called N2 (height of 14 Mm), in AR 11123. The 3D view to the left shows two sets of field lines representing the pre-reconnected lines (in blue color) and reconnected lines (in red color), as inferred from the observed evolution described in Mandrini et al. (2014b). In this panel and the one on the bottom right, the black continuous lines correspond to the photospheric trace of QSLs computed from a LFFF model. The top panel corresponds to an Atmospheric Imaging Assembly (AIA) image in the 304 Å band showing the brightenings of a confined flare that occurred on 11 November 2010 at 7:42 UT. Following the yellow and red arrows, we can see that the reconnected field lines associated to N2, with photospheric footpoints along the null separatrices, extend only along a short portion of flare brightenings. This implies that reconnection at the null point cannot explain all of the flare extension. The letters and numbers identify the different polarities in the AR. All axes are in Mm and the isocontours of the field correspond to  $\pm 50, 100$  G in continuous magenta/cyan style for the positive/negative values (magnetogram at 07:06 UT). See also Fig. 4. Adapted from Mandrini et al. (2014b).

is discontinuous, i.e. active events can be explained by magnetic reconnection in either magnetic null points or BPs and associated separatrices. In Sec. 3. we will show an example of a flare in which a null point was present but only QSLs can explain the full extension of flare brightenings. In Sec. 4. we will discuss how magnetic reconnection proceeds at QSLs using the results of MHD simulations that resemble the photospheric field distribution in ARs and, finally, in Sec. 5. we will summarize the findings in this area of research.

## 2. Solar phenomena and discontinuous magnetic field connectivity

The field connectivity in the neighbourhood of a null point displays a structure that is characterized by the so-called spines and fans (see e.g. Longcope, 2005; Pontin et al., 2011). From an observational point of view, the origin of several flares has been associated to magnetic reconnection in the fan or spine structure of null points (see e.g. Mandrini et al., 1991, 1993, 2006, 2014b; Parnell et al., 1994; Aulanier et al., 2000; Manoharan & Kundu, 2005; Luoni et al., 2007; Reid et al., 2012). Fur-

thermore, magnetic null points have been found in the global coronal magnetic field computed using potential-field source surface (PFSS) models; reconnection in their vicinity has been proposed as a way to drive the coronal plasma into the slow solar wind (van Driel-Gesztelyi et al., 2012; Mandrini et al., 2014a).

From a mathematical point of view, the neighbourhood of a magnetic null point can be described by the linear term in the local Taylor expansion of the magnetic field (see Démoulin et al., 1994, and references therein). Diagonalisation of the Jacobian field-matrix gives three eigenvectors and the corresponding eigenvalues, which add up to zero to locally satisfy the divergence-free condition on the field. Under coronal conditions, the eigenvalues are real (Lau & Finn, 1990). A positive null point has two positive fan eigenvalues and conversely for a negative null. When a null point is present, the coronal volume is divided into two connectivity domains, which are separated by the surface of the fan. In each of these domains a spine is present, separating again each volume in two others. Fig. 1 shows the magnetic connectivity in the neighborhood of a null point found in AR 10486 by Luoni et al. (2007). Two M-class homologous flares oc-

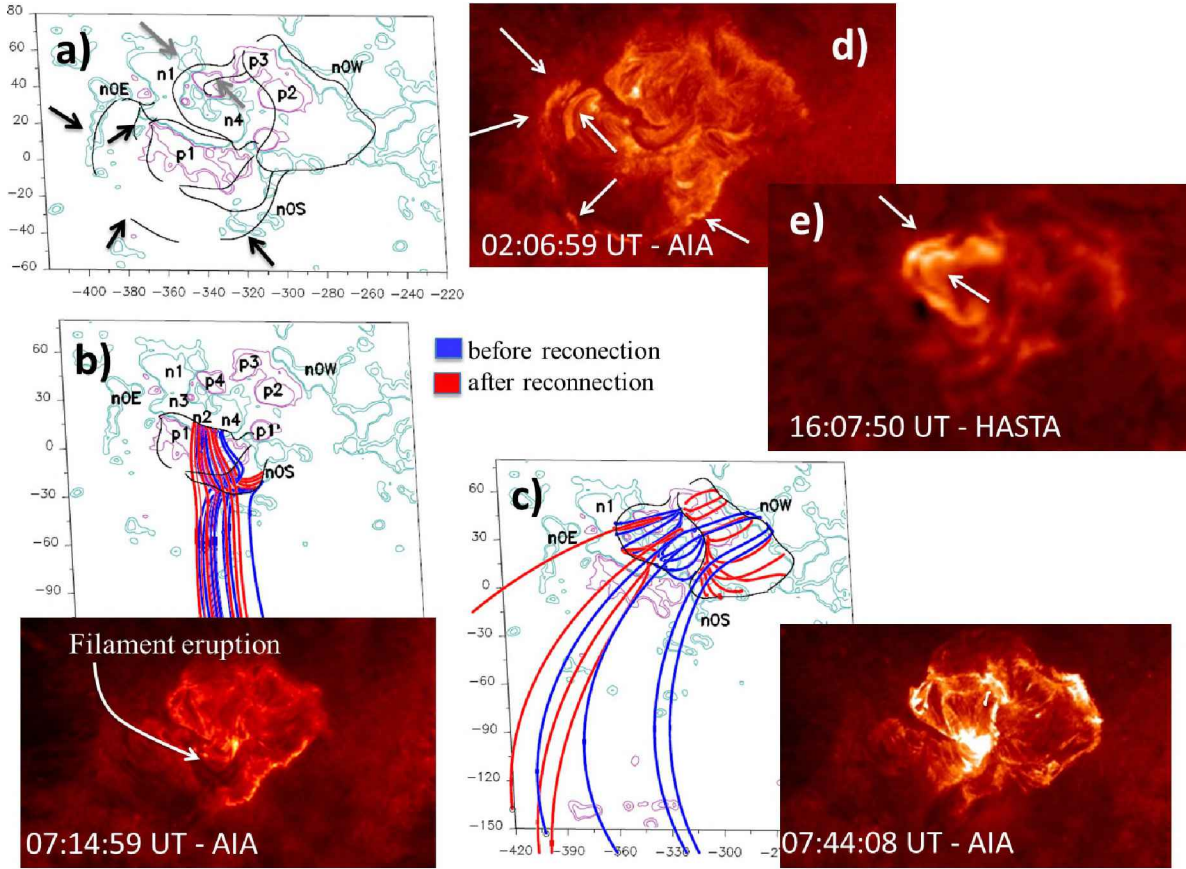


Figure 4: (a) Trace of all the QSLs on the photosphere (solid black lines) superimposed on the contours ( $\pm 50, 100$  G, magenta/cyan for positive/negative values) of the magnetic field of AR 11123 observed by the Helioseismic and Magnetic Imager on 11 November 2010. (b) Subset of QSLs associated with the ejection of a filament at the start of the flare at 07:16 UT. In red and blue, field lines with bases are shown at both sides of QSLs. By reconnection between the two sets of blue lines, the magnetic field above the filament it would be modified allowing its ejection. The red lines correspond to the lines resulting from the reconnection process. An image of AIA is shown superimposed on the field model at  $304 \text{ \AA}$ . (c) Idem panel (a) for the confined flare at 07:42 UT with an image of the same to its bottom right. (d) Brightenings corresponding to the flare at 01:58 TU observed by AIA in the  $304 \text{ \AA}$  band. (e) Brightenings of the flare at 15:53 TU observed with the H $\alpha$  Solar Telescope for Argentina (HASTA). Notice in all cases the spatial coincidence between the brightenings and the QSLs. All these QSL traces are computed using the same magnetogram (at 07:06 UT), which emphasizes that QSLs indicate the location of flare ribbons once the magnetic configuration is established. The black and grey arrows in (a) indicate which sections of the QSLs are associated with the brightenings in panels (d) and (e). The letters and numbers identify the different polarities in the AR. Adapted from Mandrini (2016). The axes of the model are in Mm.

cured at 09:21 UT and at 12:27 UT on 27 October 2003 in this active region. The different panels in Fig. 1 show the bright EUV loops for each flare and the field lines computed in the close vicinity of the null point derived from a linear force-free field (LFFF) coronal model. Notice that the shape of the field lines match closely the shape of the bright EUV loops as a proof of reconnection occurring at the null point and associated separatrices.

Apart from cases in which magnetic nulls are present, separatrices appear in magnetic configurations with BPs. Combining observations and magnetic field modelling, BPs were found associated to different kinds of events. Aulanier et al. (1998) found a close association between BP separatrices and a small flare. Delannée & Aulanier (1999) studied a flare in a BP configuration, where reconnection could have given place to a CME; while Wang et al. (2002) found elongated bright

features linked to BPs before an X-class flare and CME. Fletcher et al. (2001) studied transition region (TR) brightenings related to BPs. Mandrini et al. (2002) presented a non-classical scenario in which interacting BPs were related to the formation of arch-filament systems and a H $\alpha$  surge. Pariat et al. (2004) discussed the importance of BPs for the emergence of undulatory flux tubes and Ellerman bombs. We show in Fig. 2 the first clear example of a series blowout jets, that evolved into narrow CMEs, occurring in a BP topology in AR 10484 on 21–24 October 2003 (the figure illustrates one event). In order to explain the series of jets, some of which were accompanied by intense flares, Chandra et al. (2017) proposed that magnetic reconnection could occur at the BP separatrices forced by the destabilization of a flux rope underlying them. This process could bring the cool flux-rope material into the reconnected open field lines

driving the series of recurrent blowout jets and accompanying CMEs.

### 3. Quasi-separatrix layers and active events

Though the presence of null points and BPs can help us interpret where magnetic free energy is released in several solar phenomena, in a large number of cases, as discussed in Sec. 1., more general topological structures are needed. As an example Fig. 3 shows that if we compute field lines starting integration in the neighborhood of a null point, the footpoints of these lines lie at the intersection of the null-point separatrices with the photosphere; however, in this case the separatrix traces cover only a portion of flare brightenings implying that most of the elongated flare ribbons cannot be explained by energy release in the null point vicinity.

The original method to determine the location of QSLs was described by Démoulin et al. (1996). QSLs were defined using the norm of the Jacobian matrix of the field-line mapping; the value of the norm depends on the direction chosen to compute the mapping (positive to negative polarities or the reverse). In this case, the norm has different values at the two footpoints of a field line in the photosphere. This ambiguity in the method was solved by Titov et al. (2002), who defined the squashing degree,  $Q$ , which is independent of the mapping direction.  $Q$  is the norm squared divided by the ratio of the vertical component of the photospheric field at both ends of a field line. In this way,  $Q$  could be assigned to have a constant value along each field line.

The computation of QSLs, which in their definition include null points and BPs as extreme cases, helps to understand where flare kernels or other energy release manifestations should be found in the solar atmosphere (see e.g. Démoulin et al., 1997; Bagalá et al., 2000; Mandrini et al., 2006, 2014b, 2015; Cristiani et al., 2007; Savcheva et al., 2015; Janvier et al., 2016; Polito et al., 2017; Joshi et al., 2017; López Fuentes et al., 2018). In some of the just mentioned studies, photospheric currents derived from vector magnetograms were found at QSLs, emphasizing the role of QSLs as places where currents can build up. Fig. 4 shows an example of several flares that can be explained by reconnection at QSLs.

If the observed magnetic field structure is moderately sheared or twisted, the characteristics of QSLs in complex configurations depend strongly on the surface (i.e. photosphere) distribution of the line-of-sight field component and weakly on the details of the coronal field model. This means that QSLs are a good tool to understand where energy release will happen and to learn about the properties of energy release sites (see the reviews by Longcope, 2005; Démoulin, 2006; Mandrini, 2010).

### 4. Magnetic reconnection at QSLs

The just described examples provide a static view of the relationship between the magnetic field topology and solar active phenomena. We start with a photospheric magnetogram at a given time, in general we choose the

closest in time to the event we want to analyze. This magnetogram is taken as boundary condition to compute a coronal magnetic field model that is in general static (a potential, LFFF or non-LFFF model). The next step is to find either magnetic null points, as discussed in Sec. 2., BPs following their definition or, in a more general case, to determine the locations of QSLs. QSLs are computed by integrating an extremely high number of field lines in a very precise way. To decrease the computation time, we use an adaptive mesh to progressively refine the computation of field lines where  $Q$  has the highest values (i.e. where the connectivity changes more drastically). We follow this iterative method until the QSL is locally well resolved or when the limit of the integration precision is reached (see more details in Mandrini et al., 2015). We then compare the location of QSLs to flare brightenings and conclude on the role of any of the just mentioned topological structures as the location where reconnection occurs, i.e. we can understand where energy release happens but not how it happens or how the magnetic field evolves as it reconnects at QSLs.

To answer questions such as: are currents formed at QSLs as the magnetic field evolves before reconnection? or how do the field lines evolve when reconnection occurs at QSLs?, we need to build an MHD model of the coronal field that includes its dynamics. Aulanier et al. (2005) performed zero- $\beta$  resistive MHD simulations of the development of electric currents in magnetic configurations which were driven by smooth and large-scale sub-Alfvénic boundary motions. The magnetic configurations had QSLs in their potential state. Extended electric currents formed naturally in the configurations as well as narrow current layers at small scales all around the QSLs. For long-time motions, the strongest currents developed where the QSLs were thinnest, the region which would correspond to the generalization of the separator concept. These simulations self-consistently accounted for the long-duration energy storage prior to a flare, followed by the start of reconnection when the currents reached the dissipative scale. These results led the authors to conjecture that physically, current layers must always form at the QSL scale.

As a next step, Aulanier et al. (2006) studied the characteristics of 3D reconnection in thin QSLs. They analyzed magnetic configurations that had been weakly stressed by asymmetric line-tied twisting motions and whose potential fields already had thin QSLs. When the driving was suppressed, magnetic reconnection occurred due to the self-pinching and dissipation of narrow current layers formed previously along the QSLs. They found that a property of this reconnection process was the continuous slippage of magnetic field lines along each other, while they pass through the current layers (see also Janvier et al., 2013). This behavior is contrary to standard null point reconnection, in which field lines clearly reconnect by pairs that abruptly exchange their connectivities. These authors concluded that QSLs can physically behave as real separatrices at MHD time scales, because magnetic lines can change their connectivity on time scales much shorter than the travel-time of Alfvén waves along them.

Several MHD simulations were performed to analyze the characteristics of QSLs and the development and evolution of electric currents formed at their locations (see e.g. Janvier et al., 2014; Savcheva et al., 2012; Aulanier et al., 2010; Masson et al., 2009). Concerning observations showing evidence of slip-running reconnection, the first example was presented by Aulanier et al. (2007); while other cases were discussed (see e.g. Sobotka et al., 2016; Li & Zhang, 2015, 2014; Dudik et al., 2014; Chandra et al., 2011; Schmieder et al., 2009). Observation of this process is difficult because high-spatial and temporal resolution data are required.

## 5. Summary

We have shown that there is a close link between the magnetic field topology, understood in terms of the connectivity of its field lines, and the location where solar active phenomena occur. These locations are either regions where the magnetic field line connectivity is discontinuous (null points or BPs) or where it suffers a drastic change (QSLs). In this sense QSLs are a generalization of separatrices. We have also shown that once the photospheric configuration is set and does not evolve abruptly, we can compute QSLs and determine beforehand where we should expect that an event happens.

Furthermore, both observations and MHD simulations indicate that as the magnetic configuration evolves currents are formed at QSLs. In MHD simulations, at some point during the evolution of the modelled configuration, magnetic reconnection and the consequent energy release starts. The magnetic reconnection process is characterized by the slipping of magnetic field lines across QSLs. In this sense, clues have been found of the appearance of brightening displacements along flare ribbons that lie at QSLs. Work in this line continues both observationally and combining observations with numerical simulations.

*Acknowledgements:* CHM is a member of the Carrera del Investigador Científico (CONICET). The author thanks the Organizing Committees of the Second Binational Meeting AAA-SOCHIAS 2018 for the invitation to give the talk associated to this article and for the support received.

## References

- Aly J.J., Amari T., 1997, *A&A*, 319, 699  
 Archontis V., Hood A.W., 2013, *ApJL*, 769, L21  
 Aulanier G., Parlat E., Démoulin P., 2005, *A&A*, 444, 961  
 Aulanier G., et al., 1998, *SoPh*, 183, 369  
 Aulanier G., et al., 2000, *ApJ*, 540, 1126  
 Aulanier G., et al., 2006, *SoPh*, 238, 347  
 Aulanier G., et al., 2007, *Science*, 318, 1588  
 Aulanier G., et al., 2010, *ApJ*, 708, 314  
 Bagalá L.G., et al., 1995, *SoPh*, 161, 103  
 Bagalá L.G., et al., 2000, *A&A*, 363, 779  
 Chandra R., et al., 2011, *SoPh*, 269, 83  
 Chandra R., et al., 2017, *A&A*, 598, A41  
 Cristiani G., et al., 2007, *SoPh*, 240, 271  
 Delannée C., Aulanier G., 1999, *SoPh*, 190, 107  
 Démoulin P., 2006, *Adv. Space Res.*, 37, 1269  
 Démoulin P., Henoux J.C., Mandrini C.H., 1994, *A&A*, 285  
 Démoulin P., et al., 1996, *A&A*, 308, 643  
 Démoulin P., et al., 1997, *A&A*, 325, 305  
 Dudik J., et al., 2014, *ApJ*, 784, 144  
 Effenberger F., et al., 2011, *Physics of Plasmas*, 18, 032902  
 Fletcher L., et al., 2001, *SoPh*, 203, 255  
 Gorbachev V.S., Somov B.V., 1988, *SoPh*, 117, 77  
 Gorbachev V.S., Somov B.V., 1989, *Soviet Ast.*, 33, 57  
 Janvier M., et al., 2013, *A&A*, 555, A77  
 Janvier M., et al., 2014, *ApJ*, 788, 60  
 Janvier M., et al., 2016, *A&A*, 591, A141  
 Joshi N.C., et al., 2017, *ApJ*, 845, 26  
 Lau Y.T., Finn J.M., 1990, *ApJ*, 350, 672  
 Li T., Zhang J., 2014, *ApJL*, 791, L13  
 Li T., Zhang J., 2015, *ApJL*, 804, L8  
 Longcope D.W., 1996, *SoPh*, 169, 91  
 Longcope D.W., 2005, *Liv. Rev. Solar Phys.*, 2, 7  
 López Fuentes M., et al., 2018, *SoPh*, 293, 166  
 Luoni M.L., et al., 2007, *Adv. Space Res.*, 39, 1382  
 Mandrini C.H., 2010, A.G. Kosovichev, A.H. Andrei, J.P. Rozelot (Eds.), *Solar and Stellar Variability: Impact on Earth and Planets*, *IAU Symposium*, vol. 264, 257–266  
 Mandrini C.H., 2016, *BAAA*, 58, 256  
 Mandrini C.H., et al., 1991, *A&A*, 250, 541  
 Mandrini C.H., et al., 1993, *A&A*, 272, 609  
 Mandrini C.H., et al., 1996, *SoPh*, 168, 115  
 Mandrini C.H., et al., 1997, *SoPh*, 174, 229  
 Mandrini C.H., et al., 2002, *A&A*, 391, 317  
 Mandrini C.H., et al., 2006, *SoPh*, 238, 293  
 Mandrini C.H., et al., 2014a, *SoPh*, 289, 4151  
 Mandrini C.H., et al., 2014b, *SoPh*, 289, 2041  
 Mandrini C.H., et al., 2015, *ApJ*, 809, 73  
 Manoharan P.K., Kundu M.R., 2005, *Adv. Space Res.*, 35, 70  
 Masson S., et al., 2009, *ApJ*, 700, 559  
 Milano L.J., et al., 1999, *ApJ*, 521, 889  
 Parlat E., Aulanier G., Démoulin P., 2006, D. Barret, F. Casoli, G. Lagache, A. Lecavelier, L. Pagani (Eds.), *SF2A-2006: Semaine de l'Astrophysique Française*, 559  
 Parlat E., Masson S., Aulanier G., 2009, *ApJ*, 701, 1911  
 Parlat E., et al., 2004, *ApJ*, 614, 1099  
 Parnell C.E., Priest E.R., Golub L., 1994, *SoPh*, 151, 57  
 Polito V., et al., 2017, *A&A*, 601, A39  
 Pontin D.I., Al-Hachami A.K., Galsgaard K., 2011, *A&A*, 533, A78  
 Reid H.A.S., et al., 2012, *A&A*, 547, A52  
 Savcheva A., et al., 2012, *ApJ*, 750, 15  
 Savcheva A., et al., 2015, *ApJ*, 810, 96  
 Schmieder B., et al., 2007, *Adv. Space Res.*, 39, 1840  
 Schmieder B., et al., 2009, *Earth, Planets, and Space*, 61, 565  
 Sobotka M., et al., 2016, *A&A*, 596, A1  
 Sweet P.A., 1958, B. Lehnert (Ed.), *Electromagnetic Phenomena in Cosmical Physics*, *IAU Symposium*, vol. 6, 123  
 Sweet P.A., 1969, *ARA&A*, 7, 149  
 Syrovatskii S.I., 1981, *ARA&A*, 19, 163  
 Takasao S., et al., 2015, *ApJ*, 813, 112  
 Titov V.S., Hornig G., Démoulin P., 2002, *Journal of Geophysical Research (Space Physics)*, 107, 1164  
 Titov V.S., Priest E.R., Démoulin P., 1993, *A&A*, 276, 564  
 van Driel-Gesztelyi L., et al., 2012, *SoPh*, 281, 237  
 Vekstein G., Priest E.R., Amari T., 1991, *A&A*, 243, 492  
 Wang T., et al., 2002, *ApJ*, 572, 580  
 Wilmot-Smith A., Hornig G., Pontin D.I., 2009, *ApJ*, 696, 1339